INTERNATIONAL JOURNAL FOR NUMERICAL METHODS IN FLUIDS, VOL. 20, 1111–1136 (1995)

SIMULATION OF 2D EXTERNAL VISCOUS FLOWS BY MEANS OF A DOMAIN DECOMPOSITION METHOD USING AN INFLUENCE MATRIX TECHNIQUE

WEN-ZHONG SHEN AND TA PHUOC LOC
LIMSI-CNRS, BP 133, F-91403 Orsay Cedex, France

SUMMARY

Two-dimensional external viscous flows are numerically approximated by means of a domain decomposition method which combines a vortex method and a finite difference method. The vortex method is used in the flow region which is dominated by convective effects, whereas the finite difference method is used in the flow region where viscous diffusion effects are dominant. An influence matrix technique combined with the uniformity condition of the pressure is used to enforce the tangential velocity boundary condition. Comparisons between numerical and experimental data show that the method is well adapted for simulating two-dimensional flows.

KEY WORDS domain decomposition method; finite difference method; vortex method; influence matrix technique; Navier–Stokes equations; incompressible viscous flows

1. INTRODUCTION

The domain decomposition method is very commonly used in the spectral,[1] finite element[2] and spectral–finite element[3] methods. In the vortex method, Cottet[4] uses a domain decomposition method with overlapping coupled with the finite difference method. In References 5–7 we use a domain decomposition method of Schur complement coupled also with the finite difference method. In the finite difference method with the formulation (ψ, ω) we often use a Dirichlet boundary condition for the vorticity in which the tangential velocity boundary condition is imposed. Numerically this discretization gives a satisfactory result, but mathematically it is insufficient because the converse is not true, i.e. the tangential velocity calculated with this Dirichlet boundary condition is no longer zero.

To overcome the difficulty involved in this coupling at the boundary, an influence matrix technique is presented. The influence matrix technique, also known as the capacitance matrix technique, has been widely used to solve systems of elliptic linear equations in situations with irregular boundaries,[8–11] unavailable boundary conditions[12] or coupled boundary conditions for components of variables.[13] In all cases the technique makes use of the principle of superposition of solutions to elementary problems. A linear combination of these elementary solutions is then sought in order to ensure an additional condition.

Kleiser and Schumann[14] were apparently the first to use the influence matrix technique for the incompressible Navier–Stokes equations in primitive variables in 3D. Later this technique was extended by Le Quéré and Alziary de Roquefort[12,15] to 2D problems.

CCC 0271–2091/95/101111–26

Received February 1994
Revised June 1994

For the Navier–Stokes equations in non-primitive variables the influence matrix technique was also used to overcome the boundary condition for ω. When solving the 2D Navier–Stokes equations formulated in terms of the velocity function $\vec{u}$ and vorticity function ω, the influence matrix expresses a linear relationship between the distribution of vorticity and the divergence of velocity along the boundary.[16] In terms of the streamfunction ψ and vorticity ω,[17–19] the influence matrix gives a linear relationship between the vorticity and the tangential velocity at the boundary.

It is noted that the streamfunction at the boundary was assumed known. However, in the case of external flow this function must be determined.

In this paper an influence matrix method coupled with the uniformity condition of the pressure is proposed to solve 2D external incompressible viscous flows. This finite difference method is coupled with a vortex method. Numerical evidence of the efficiency of the present method is supported by the simulation of the flow around an aerofoil with incidences of 34° and 20° at Reynolds numbers of 1000 and 10,000.

2. DOMAIN DECOMPOSITION METHOD

We use a domain decomposition method[1,2] here to simulate the external viscous flows around an obstacle. The fluid domain $\mathscr{D}$ is decomposed into two open subdomains so that $\mathscr{D} = \mathscr{D}_0 \cup \overline{\mathscr{D}_1}$, where $\mathscr{D}_1$ is homeomorphic with a disc. Thus the convective effects are dominant in $\mathscr{D}_0$ and a particle method is used. In the subdomain $\mathscr{D}_1$, the viscous effects are dominant and a finite difference method is used. Let B_1 (resp. Γ_1) be the interface between $\mathscr{D}_1$ and the obstacle (resp. $\mathscr{D}_0$) and let n_i be the outward normal to the boundary of $\mathscr{D}_i$ for $i=0$, 1 (see Figure 1).

In $\mathscr{D}_0$ the Navier–Stokes equations are formulated in terms of the velocity and vorticity $(\vec{u}_0, \omega)$ as

$$\frac{\partial \omega_0}{\partial t} + \nabla \cdot (\omega_0 \vec{u}_0) = \frac{2}{Re} \nabla^2 \omega_0, \tag{1}$$

$$\operatorname{curl} \vec{u}_0 = \omega_0 \vec{k}, \tag{2}$$

$$\nabla \cdot \vec{u}_0 = 0, \tag{3}$$

$$\vec{u}_0 \to U_\infty \vec{i} \quad \text{at infinity}, \tag{4}$$

in which all quantities have been normalized by the half-chord of the profile a and the velocity U_∞. The Reynolds number is defined by $Re = U_\infty 2a/\nu$.

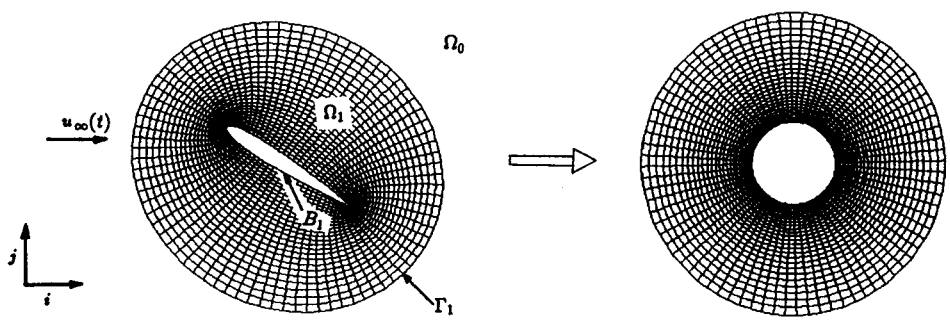

Figure 1. Definition of computational domain and subdomains

In $\mathscr{D}_1$ they are formulated in terms of the vorticity and streamfunction as

$$\frac{\partial \omega}{\partial t} + \nabla \cdot \left[\omega \nabla \times \left(\psi \vec{k}\right)\right] = \frac{2}{Re} \nabla^2 \omega, \tag{5}$$

$$\nabla^2 \psi = -\omega. \tag{6}$$

At the wall the boundary conditions for the vorticity and the constant value of the streamfunction are calculated by an influence matrix technique and the uniformity condition of the pressure, $\oint (\partial \omega / \partial \vec{n}_1) = 0$. The condition at infinity is treated naturally by the particle method (Biot–Savart law).

Let $T_t > 0$ and N be a positive integer; the Navier–Stokes problem is to be solved in the time interval $[0, T_t]$. Let $\delta t = T_t / N$ and $t_k = k\delta t$ with $0 \leq k \leq N$. Assume that the solutions are known in time intervals (t_{l-1}, t_l) so that $1 \leq l \leq k < N$. We will solve the system in time intervals (t_k, t_{k+1}).

2.1. *Particle method in $\mathscr{D}_0$*

The fluid motion is studied in the reference frame of the obstacle. In $\mathscr{D}_0$ the advection–diffusion equation of ω_0 is approximated by

$$\frac{\partial \omega_0^{k+1}}{\partial t} + \nabla \cdot \left(\omega_0^{k+1} \vec{u}_0^k\right) = \frac{2}{Re} \nabla^2 \omega_0^{k+1}, \tag{7}$$

in which the velocity field is given by the Green identity

$$\vec{u}_0^k(\vec{x}) = U_\infty \vec{i} + \int_{\mathscr{D}_0 \cup \mathscr{D}_1} \omega^k \nabla G(\vec{y} - \vec{x}) \times \vec{k} \, \mathrm{d}v, \tag{8}$$

where $G(\vec{y} - \vec{x}) = (1/2\pi) \log|\vec{y} - \vec{x}|$ is the Green function of the Laplace operator in $\mathbb{R}^2$.

The problem is completely defined with some transmission conditions. For high Reynolds numbers equation (7) can be locally considered as a hyperbolic equation whose right-hand side, $(2/Re)\nabla^2 \omega_0^{k+1}$, is a perturbation. For this kind of problem Dirichlet conditions are imposed on the subset of Γ_1 where the flow enters $\mathscr{D}_0$. In this framework the transmission conditions that are needed can be expressed as

$$\omega_0^{k+1}(\vec{x}) = \omega_1^k(\vec{x}) \quad \text{if} \quad \vec{u}_0^k(\vec{x}) \cdot \vec{n}_0(\vec{x}) < 0. \tag{9}$$

The problem presented above is approximated by means of a particle method that can take account of Dirichlet data. All details may be found in Reference 5.

2.2. *Finite difference method in $\mathscr{D}_1$*

In subdomain $\mathscr{D}_1$ the Navier–Stokes equations are derived using the streamfunction–vorticity formulation. As usual with the influence matrix technique, we use a semi-implicit Adams–Basforth–Crank–Nicolson (ABCN) scheme to advance in time. This consists of writing the transport equation (5) at the time level $(k + \frac{1}{2})\delta t$ and evaluating the diffusion term implicitly and convective terms

explicitly at this time level by means of the Adams–Bashforth extrapolation. Thus a Helmholtz equation has to be solved together with the Poisson equation and the no-slip condition. Then the system of Navier–Stokes equations becomes

$$(\sigma I - \nabla^2)\omega_1^{k+1} = S^k, \tag{10}$$

$$\nabla^2 \psi_1^{k+1} = -\omega_1^{k+1}, \tag{11}$$

$$\frac{\partial \psi_1^{k+1}}{\partial \vec{n}_1} = 0 \quad \text{on } B_1, \tag{12}$$

$$\psi_1^{k+1} = \text{const.} \quad \text{on } B_1, \tag{13}$$

$$\oint \frac{\partial \omega_1^{k+1}}{\partial \vec{n}_1} = 0 \quad \text{on } B_1, \tag{14}$$

in which

$$\sigma = \frac{2Re}{\delta t}, \tag{15}$$

$$S^k = (\sigma I + \nabla^2)\omega_1^k - Re\left[3\nabla \cdot \left(\omega_1^k \nabla \times \psi_1^k \vec{k}\right) - \nabla \cdot \left(\omega_1^{k-1} \nabla \times \psi_1^{k-1} \vec{k}\right)\right]. \tag{16}$$

For the vorticity boundary conditions on B_1 we use an influence matrix technique in which the condition (12) has been considered. The uniformity condition of the pressure (14) is used to determine the streamfunction boundary value. (See Sections 3 and 4.)

The problem is well posed with the transmission conditions on Γ_1. For the streamfunction ψ we need the transmission conditions on the whole interface, because ψ is the solution of the elliptic equations (6) or (11). The condition of ψ_1^{k+1} is calculated by the formula

$$\psi_1^{k+1}(\vec{x}) = U_\infty y + \int_{\mathscr{D}_0 \cup \mathscr{D}_1} \omega^k G(\vec{x} - \vec{x}')\mathrm{d}x' - \int_{B_1} \psi^{k+1} \frac{\partial G}{\partial \vec{n}_1}(\vec{x} - \vec{x}')\mathrm{d}x'. \tag{17}$$

For the vorticity on Γ_1 the equation is considered as an elliptic equation by the finite difference method. However, the nature of the fluid flow is hyperbolic (i.e. the convective effects are dominant on the interface). Thus one calculates the vorticity conditions upon the velocity on the interface. These transmission conditions are given as

$$\omega_1^{k+1}(\vec{x}) = \omega_0^k(\vec{x} - \delta t \vec{u}^k) + \nu \delta t \nabla^2 \omega_0^k(\vec{x} - \delta t \vec{u}^k) \quad \text{if } \vec{u}^k \cdot \vec{n}_1 \leq 0, \tag{18}$$

$$\omega_1^{k+1}(\vec{x}) = \omega_1^k(\vec{x} - \delta t \vec{u}^k) + \nu \delta t \nabla^2 \omega_1^k(\vec{x} - \delta t \vec{u}^k) \quad \text{if } \vec{u}^k \cdot \vec{n}_1 \geq 0. \tag{19}$$

3. THE FIRST INFLUENCE MATRIX TECHNIQUE

3.1. The superposition principle

As known, the influence matrix method is based on the superposition principle for linear problems. Now we split the linear problem of Section 2.2 into several linear problems that can be solved easily.

Let ω_{B_1} be a given function on B_1 and consider the linear problem

$$(\sigma I - \nabla^2)\tilde{\omega} = S, \tag{20}$$

$$\tilde{\omega} = \omega_{B_1} \quad \text{on } B_1, \tag{21}$$

$$\nabla^2\tilde{\psi} = -\tilde{\omega}, \tag{22}$$

$$\tilde{\psi} = \psi_{B_1} \quad \text{on } B_1, \tag{23}$$

in which one assumes ψ_{B_1} a function well known. This problem has a unique solution $(\tilde{\omega}, \tilde{\psi})$ for an arbitrary function ω_{B_1}. If we consider the difference between this solution $(\tilde{\omega}, \tilde{\psi})$ and the solution of the problem in Section 2.2 (ω_1, ψ_1), then we have the homogeneous linear system

$$(\sigma I - \nabla^2)(\tilde{\omega} - \omega_1) = 0, \tag{24}$$

$$\tilde{\omega} - \omega_1 = \omega_{B_1} - \omega_1|_{B_1} \quad \text{on } B_1, \tag{25}$$

$$\nabla^2\left(\tilde{\psi} - \psi_1\right) = -(\tilde{\omega} - \omega_1), \tag{26}$$

$$\tilde{\psi} - \psi_1 = 0 \quad \text{on } B_1. \tag{27}$$

Let us assume that a grid in the domain near the wall is generated and N denotes the number of points lying along the boundary. Then the solution of the linear system above becomes a linear combination of the N elementary solutions defined by

$$(\sigma I - \nabla^2)\omega^k = 0, \tag{28}$$

$$\omega^k(B^j) = \delta_{kj} \quad \forall B^j \in B_1, \tag{29}$$

$$\nabla^2\psi^k = \omega^k, \tag{30}$$

$$\psi^k = 0 \quad \text{on } B_1, \tag{31}$$

where δ_{kj} is the Kronecker symbol. Each of these linear problems has a unique solution which is independent of time and can be solved once only at an early stage.

Thus the solution of the Navier–Stokes equations in $\mathscr{D}_1$ takes the form

$$\omega_1 = \tilde{\omega} + \sum_{k=1}^{N} \lambda_k \omega^k, \tag{32}$$

$$\psi_1 = \tilde{\psi} + \sum_{k=1}^{N} \lambda_k \psi^k. \tag{33}$$

According to the definition of the function ω^k, the coefficients $(\lambda_k)_{k=1,1114\ldots,1114N}$ are related to the vorticity ω_1 on the boundary B_1 by

$$\omega_1(B^k) = \tilde{\omega}(B^k) + \lambda_k \quad \forall B^k \in B_1. \tag{34}$$

The remaining work is to determine these coefficients in order to satisfy the tangential velocity boundary condition and the uniformity condition of the pressure.

3.2. *Construction of the influence matrix*

The coefficients λ_k are computed in order to ensure the tangential velocity boundary condition which is not yet taken into account. We obtain the tangential velocity relation at the boundary by differentiating relation (33) with respect to n_1 to give

$$\frac{\partial \psi_1}{\partial \vec{n}_1}(B^j) = \frac{\partial \tilde{\psi}}{\partial \vec{n}_1}(B^j) + \sum_{k=1}^{N} \lambda_k \frac{\partial \psi^k}{\partial \vec{n}_1}(B^j) \quad \forall j = 1, \ldots, N. \tag{35}$$

This equation can be written in matrix form as

$$A\lambda = f. \tag{36}$$

The elements a_{ij} of the matrix A of order N are defined by

$$a_{ij} = \frac{\partial \psi^j}{\partial \vec{n}_1}(B_i), \quad i, j = 1, \ldots, N, \tag{37}$$

and the elements f_i of the vector f are defined by

$$f_i = -\frac{\partial \tilde{\psi}}{\partial \vec{n}_1}(B_i), \quad i = 1, \ldots, N. \tag{38}$$

The matrix A is diagonally dominant because it is calculated with the elementary solutions. Then the inverse of matrix A is obtained using a GMRES (generalized minimal residual algorithm) iteration method.[2,20] If we choose the function ω_{B_1} as being equal to the value of the previous step, the GMRES iteration method converges in five iterations for a residual reduction of 10^{-4}.

3.3. *Uniformity condition of the pressure at the wall*

In the problem of Section 2.2 the streamfunction at the wall, which is constant, remains unknown. In order to determine this constant, we have the uniformity condition of the pressure (14) which is not yet taken into account. Thus we take this condition into the following discrete form using the Taylor development of series of fourth order:

$$\psi_1|_{B_1} = \frac{\sum_{j=1}^{N} [16\psi_1(2, j) - \psi_1(3, j) - 6\delta x^2 \omega_1(1, j)]}{15N}. \tag{39}$$

It is noticed that if the value of the streamfunction at the boundary changes, the old value of ω_{B_1} calculated by the influence matrix method no longer satisfies the tangential velocity boundary condition. Hence in order to satisfy these two conditions, an iteration technique is required to obtain $(\psi_{B_1}, \omega_{B_1})$.

We remark that this iteration method converges very slowly. To overcome this difficulty, we use a relaxation method to calculate the streamfunction boundary value as

$$\psi_{B_1} = \alpha \psi_{\text{old}} + (1 - \alpha)\psi_{\text{new}}. \tag{40}$$

In practice we choose $\alpha < 0$ in order to accelerate the convergence.

4. THE SECOND INFLUENCE MATRIX TECHNIQUE

In this section we add the uniformity condition of the pressure into the influence matrix. This means that we split the linear problem of Section 2.2 as in Section 3 and treat the streamfunction at the boundary in the influence matrix as unknown.

Let $(\omega_{B_1}, \psi_{B_1})$ be a given function on B_1 and consider first the problem

$$(\sigma I - \nabla^2)\tilde{\omega} = S, \tag{41}$$

$$\tilde{\omega} = \omega_{B_1} \quad \text{on } B_1, \tag{42}$$

$$\nabla^2\tilde{\psi} = -\tilde{\omega}, \tag{43}$$

$$\tilde{\psi} = \psi_{B_1} \quad \text{on } B_1. \tag{44}$$

This problem has a unique solution $(\tilde{\omega}, \tilde{\psi})$ for the arbitrary function $(\omega_{B_1}, \psi_{B_1})$. We now compare this solution with the solution of the problem in Section 2.2. We obtain a homogeneous linear system for the difference between these two solutions. Then we can build $N+1$ elementary solutions defined as

$$(\sigma I - \nabla^2)\omega^k = 0, \tag{45}$$

$$\omega^k(B^j) = \delta_{kj} \quad \forall B^j \in B_1, \tag{46}$$

$$\nabla^2\psi^k = \omega^k, \tag{47}$$

$$\psi^k = 0 \quad \text{on } B_1 \tag{48}$$

and

$$(\sigma I - \nabla^2)\omega^{N+1} = 0, \tag{49}$$

$$\omega^{N+1}(B^j) = 0 \quad \forall B^j \in B_1, \tag{50}$$

$$\nabla^2\psi^{N+1} = \omega^{N+1}, \tag{51}$$

$$\psi^{N+1} = 1 \quad \text{on } B_1. \tag{52}$$

Each of these $N+1$ linear problems has a unique solution which is also independent of time and can be solved once only at an early stage.

Thus the solution of the Navier–Stokes equations in $\mathscr{D}_1$ becomes

$$\omega_1 = \tilde{\omega} + \sum_{k=1}^{N} \lambda_k \omega^k + c\omega^{N+1}, \tag{53}$$

$$\psi_1 = \tilde{\psi} + \sum_{k=1}^{N} \lambda_k \psi^k + c\psi^{N+1}. \tag{54}$$

We now build the influence matrix using the tangential velocity boundary condition and the uniformity condition of the pressure:

$$\frac{\partial\psi_1}{\partial\vec{n}_1}(B^j) = \frac{\partial\tilde{\psi}}{\partial\vec{n}_1}(B^j) + \sum_{k=1}^{N} \lambda_k \frac{\partial\psi^k}{\partial\vec{n}_1}(B^j) + c\frac{\partial\psi^{N+1}}{\partial\vec{n}_1}(B^j) \quad \forall j = 1, \ldots, N, \tag{55}$$

$$\oint \frac{\partial \omega_1}{\partial \vec{n}_1} = \oint \frac{\partial \tilde{\omega}}{\partial \vec{n}_1} + \sum_{k=1}^{N} \lambda_k \oint \frac{\partial \omega^k}{\partial \vec{n}_1} + c \oint \frac{\partial \omega^{N+1}}{\partial \vec{n}_1} = 0. \tag{56}$$

Then we have an $(N+1) \times (N+1)$ matrix system that can determine the $(N+1)$ unknowns (λ^k, c). This matrix is not diagonally dominant, because $\oint (\partial \omega^{N+1}/\partial \vec{n}_1) = 0$. Then we use a Gauss direct method to calculate the inverse of the matrix.

We remark that we obtain the boundary values of $(\omega_{B_1}, \psi_{B_1})$ by solving the influence matrix once only. With this scheme we can reduce the computer time cost.

5. NUMERICAL IMPLEMENTATION OF THE FINITE DIFFERENCE METHOD

The system of equations is discretized in space with a second-order centred difference scheme. Then we obtain a matrix of the system which is diagonally dominant and can be solved easily by the GMRES iterative method or an alternating direction implicit (ADI) method.

For the determination of the velocity at the boundary there exist several approximation formulae. We discuss two types of discretization. A first discretization is defined by using the streamfunction only as

$$\frac{\partial \psi}{\partial x}(1, j) = \frac{18\psi(2, j) - 9\psi(3, j) + 2\psi(4, j) - 11\psi(1, j)}{6\delta x}. \tag{57}$$

This discretization is of order three. At low Reynolds numbers this scheme gives a satisfactory result. At high Reynolds numbers the scheme needs a very fine grid because the vorticity diffusion is very small, while the vorticity convection term becomes important. A strong coupling of vorticity and velocity is essential. For this reason we introduce another type of discretization that is linked to the vorticity:

$$\frac{\partial \psi}{\partial x}(1, j) = \frac{8\psi(2, j) - 7\psi(1, j) - \psi(3, j)}{6\delta x} - \frac{\delta x F(1, j)\omega(1, j)}{3}. \tag{58}$$

This discretization is also of order three and gives a very satisfactory result for all Reynolds numbers.

In the second influence matrix technique $\partial\omega/\partial x$ is also discretized with the third-order-accurate relation

$$\frac{\partial \omega}{\partial x}(1, j) = \frac{18\omega(2, j) - 9\omega(3, j) + 2\omega(4, j) - 11\omega(1, j)}{6\delta x}. \tag{59}$$

6. NUMERICAL RESULTS

The purpose of this section is to illustrate the present method in the case of unsteady flow around the NACA 0012 aerofoil at Reynolds number of 10^3 and 10^4. The domain outside the aerofoil is mapped by a conformal mapping onto the exterior of a circle, which in turn is mapped by an exponential mapping onto a semi-infinite strip $[0, \infty] \times [0, 2]$. This semi-infinite strip is decomposed into two subdomains: the 'finite difference' subdomain and the 'particle' subdomain. In the plane of the circle the 'finite difference' subdomain is limited to a ring of adimensional radius 3·6 (Figure 1).

6.1. Re = 1000

For this Reynolds number the calculations have made with an incidence of 34°. This choice is guided by the existence of numerous numerical results and experimental visualizations in the literature, necessary for our comparisons. The two influence matrix techniques described above have been

employed. They give similar results. However, the second technique is more efficient. The "finite difference' subdomain has been discretized by several grid systems (51×81, 51×121, 51×161). Numerical results reported in this paper correspond to a grid of 51×161 nodes. The time step is taken equal to 0·002. Figures 2–11 show comparisons of the flow structure between the present results and those reported in Reference 21. The comparisons show good agreement. The time evolution of the flow structure is correctly reproduced. All main and secondary vortices detected by experimental visualization are captured by numerical simulation. To illustrate the vorticity field, an example of a result obtained at $t = 12$ is given in Plate 1.

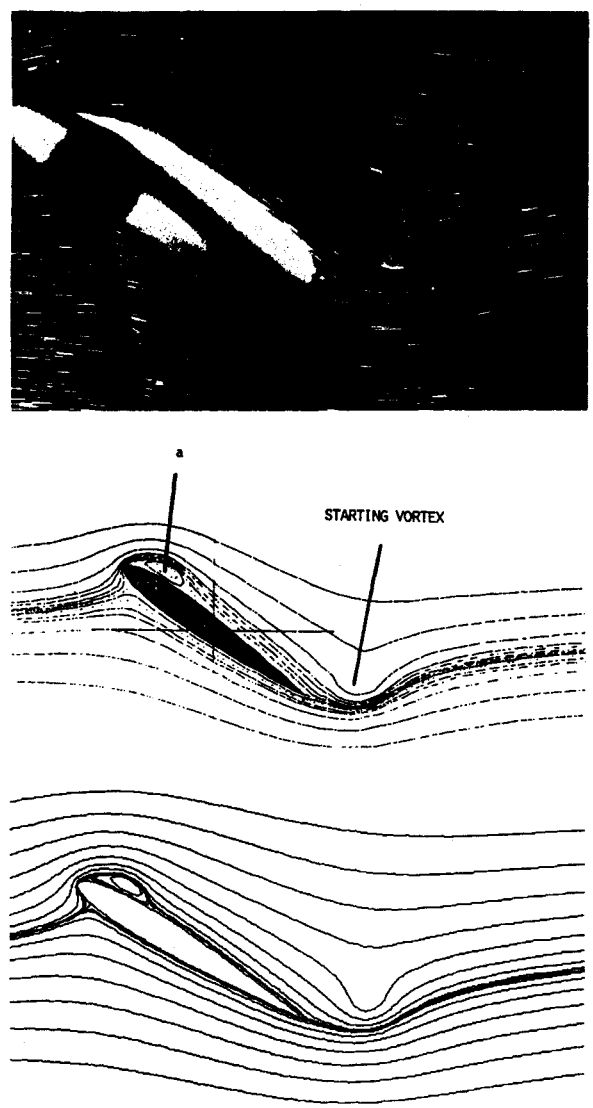

Figure 2. Comparison of flow structure between experimental visualization[21] and numerical results, $Re = 10^3$, $t = 0{\cdot}8$

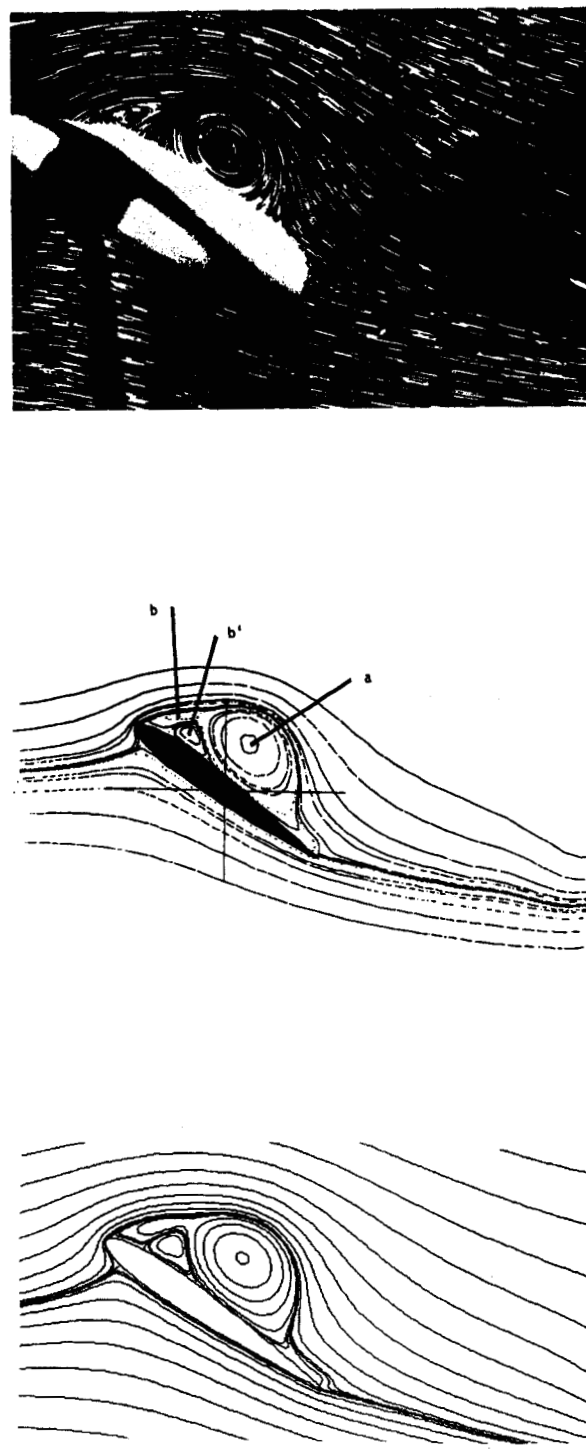

Figure 3. Comparison of flow structure between experimental visualization[21] and numerical results, $Re = 10^3$, $t = 3{\cdot}2$

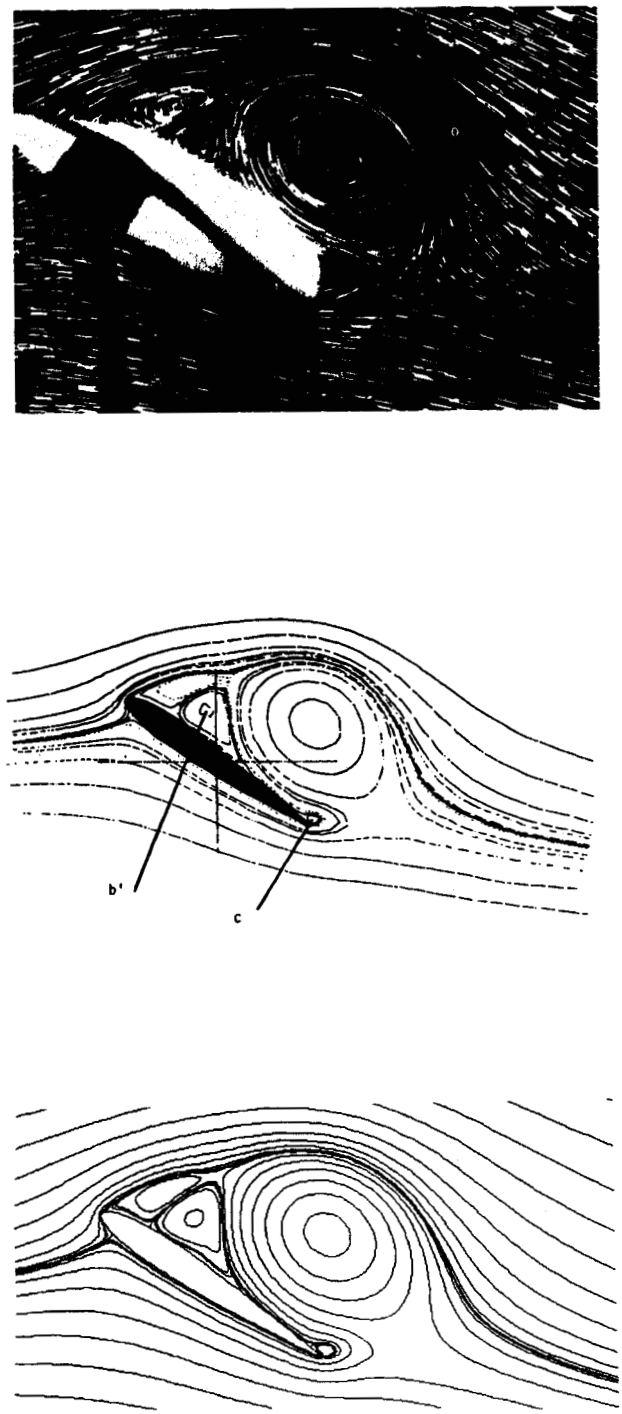

Figure 4. Comparison of flow structure between experimental visualization[21] and numerical results, $Re = 10^3$, $t = 5{\cdot}6$

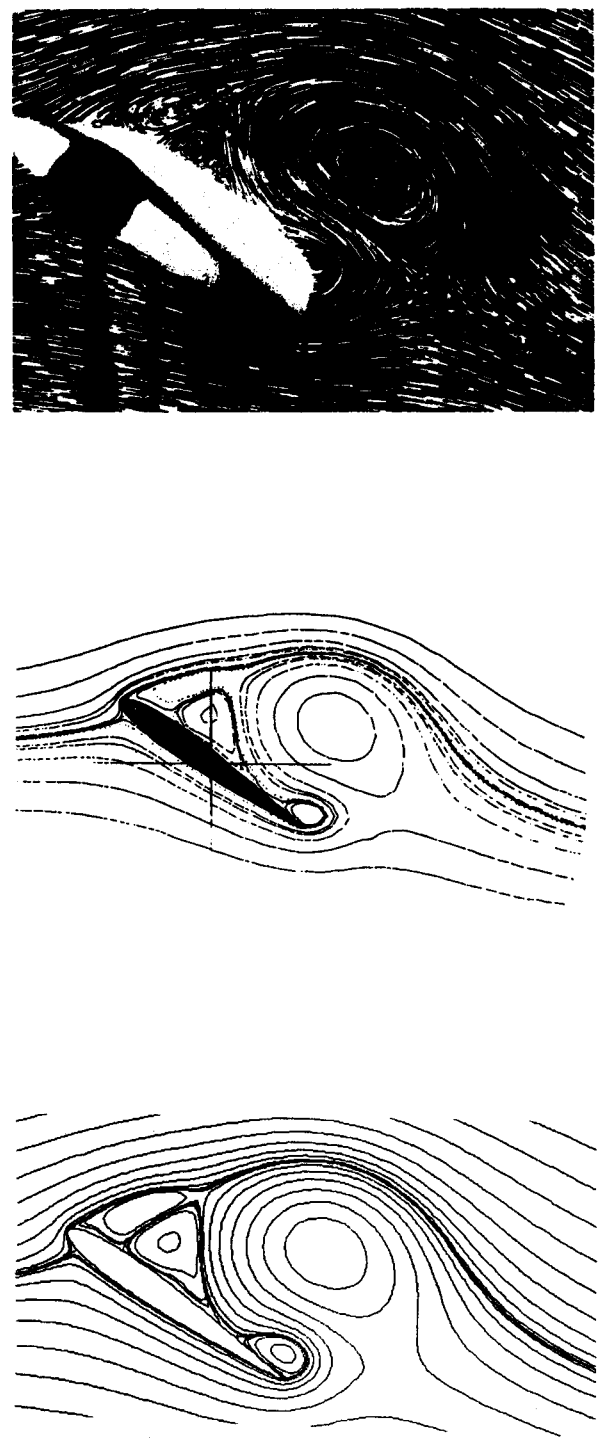

Figure 5. Comparison of flow structure between experimental visualization[21] and numerical results, $Re = 10^3$, $t = 6{\cdot}4$

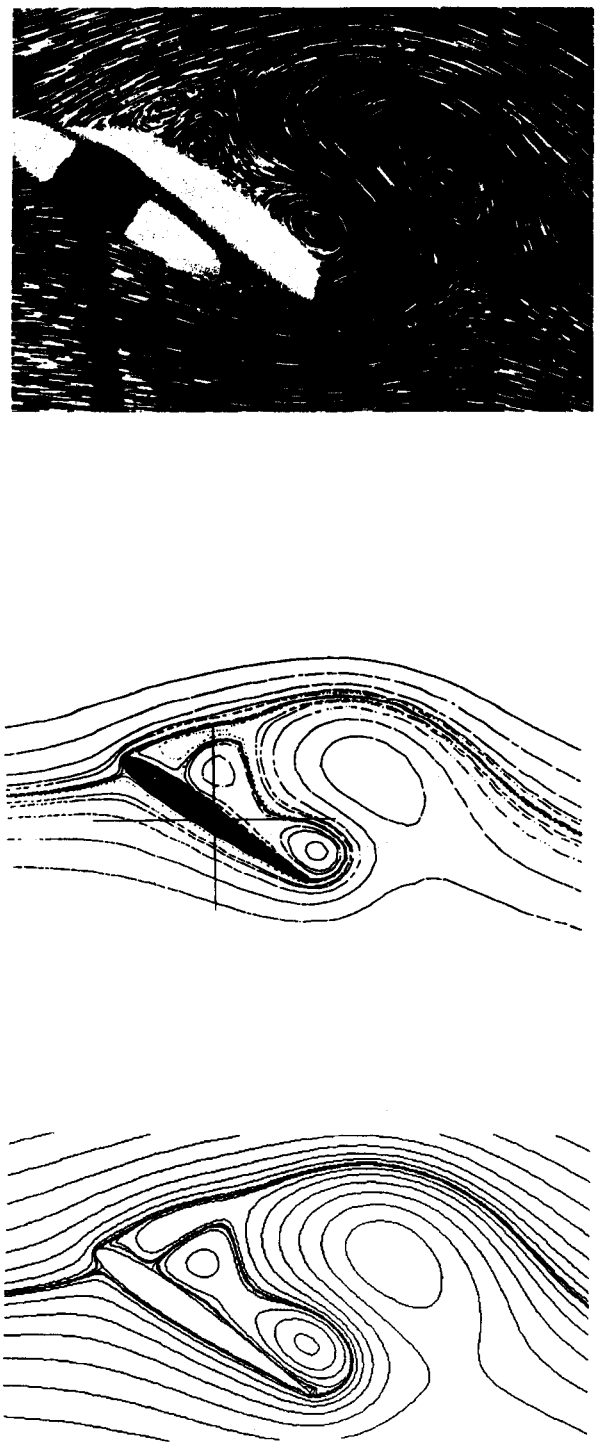

Figure 6. Comparison of flow structure between experimental visualization[21] and numerical results, $Re = 10^3$, $t = 7{\cdot}2$

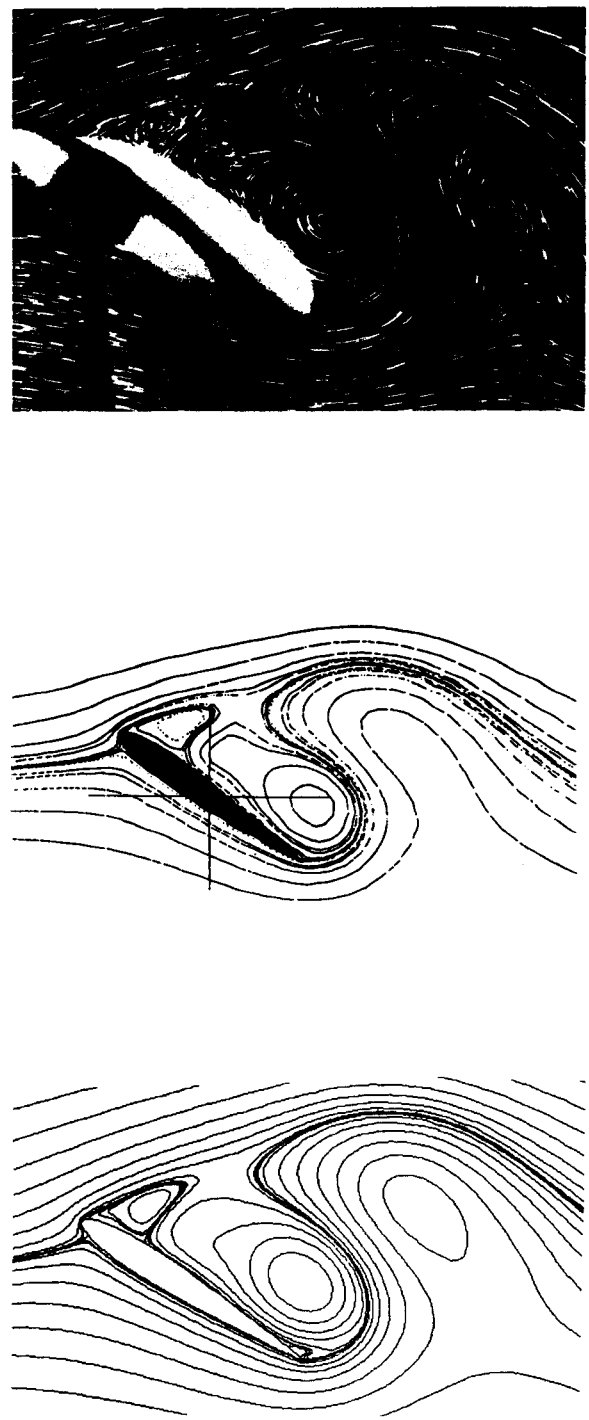

Figure 7. Comparison of flow structure between experimental visualization[21] and numerical results, $Re = 10^3$, $t = 8{\cdot}0$

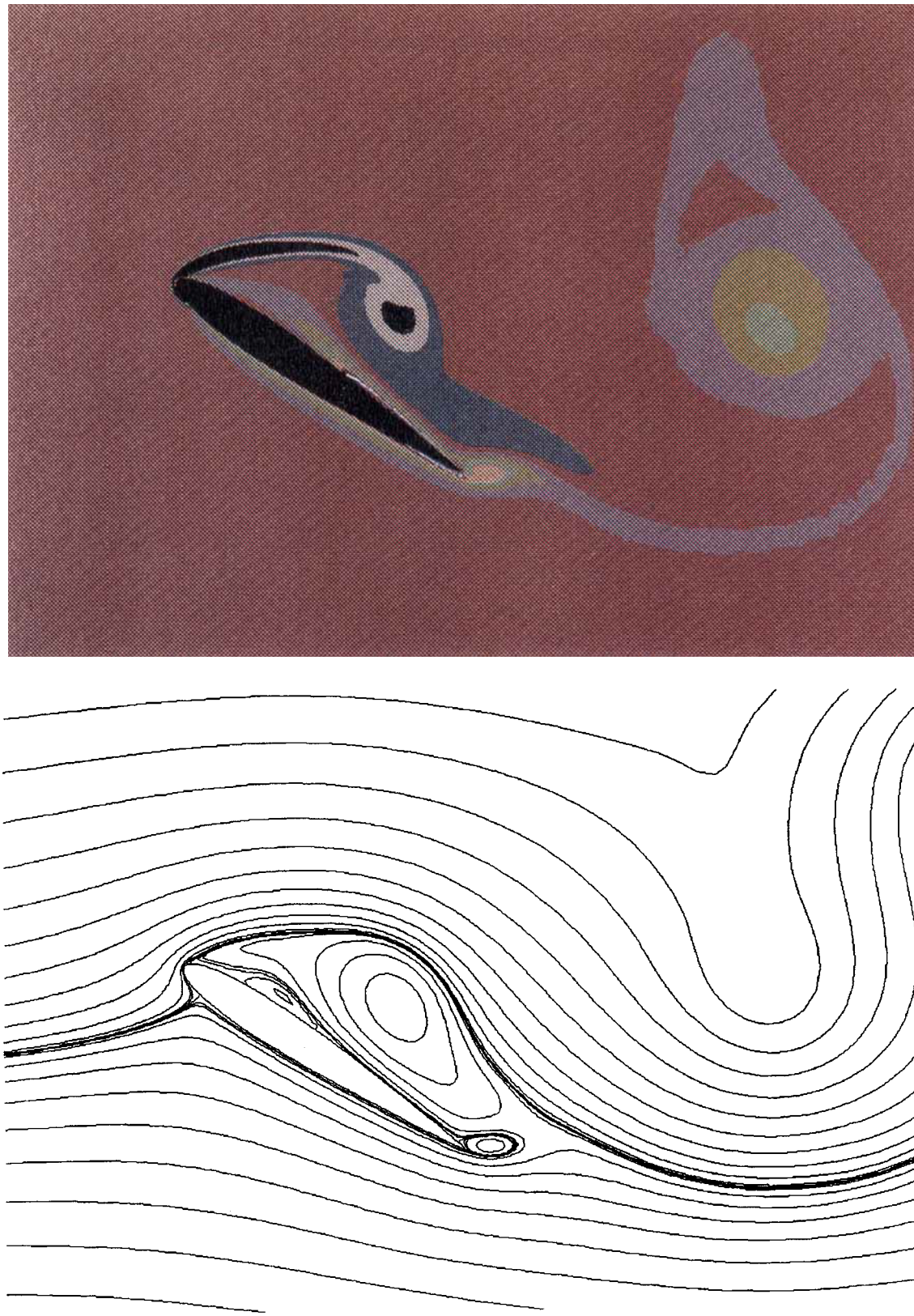

Plate 1. Vorticity field and streamlines, $Re = 10^3$, $\alpha = 34°$, $t = 12$

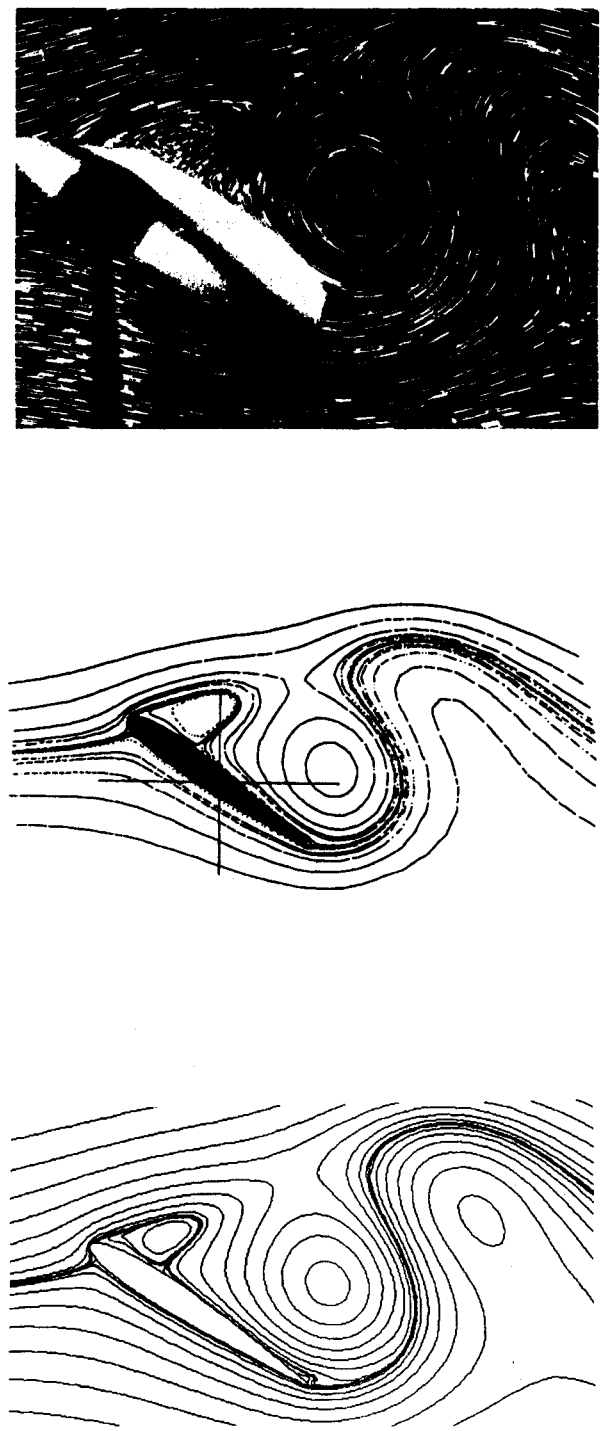

Figure 8. Comparison of flow structure between experimental visualization[21] and numerical results, $Re = 10^3$, $t = 8{\cdot}8$

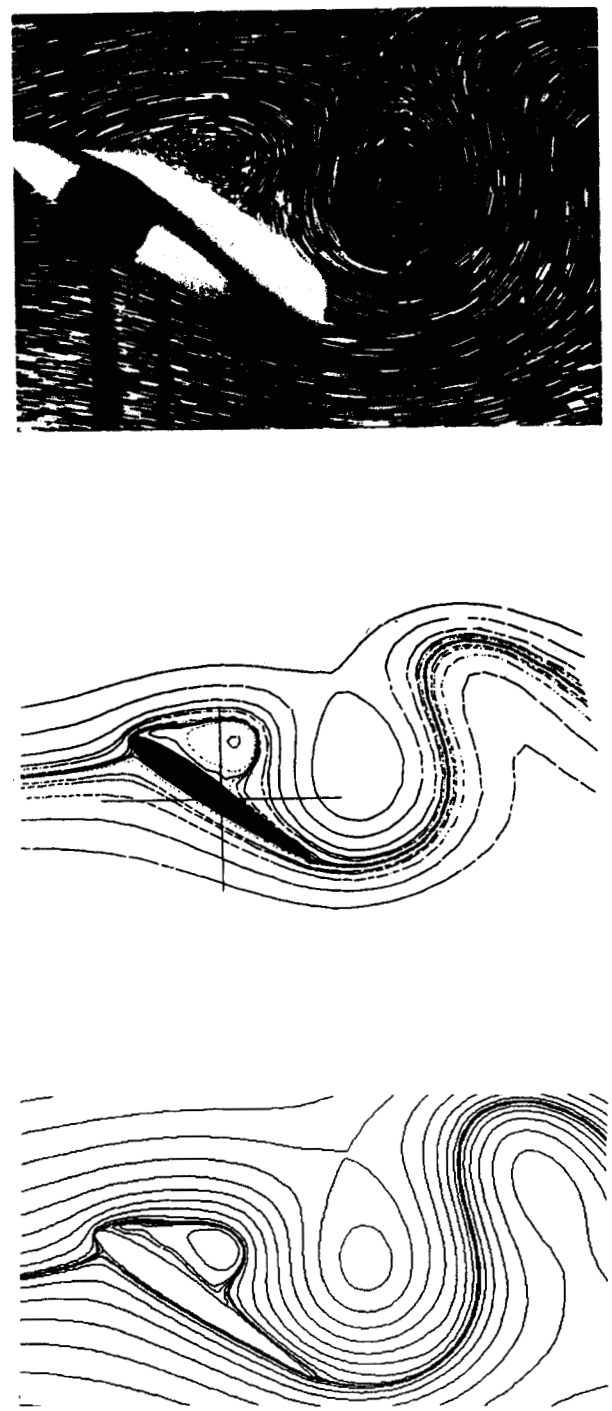

Figure 9. Comparison of flow structure between experimental visualization[21] and numerical results, $Re = 10^3$, $t = 9{\cdot}6$

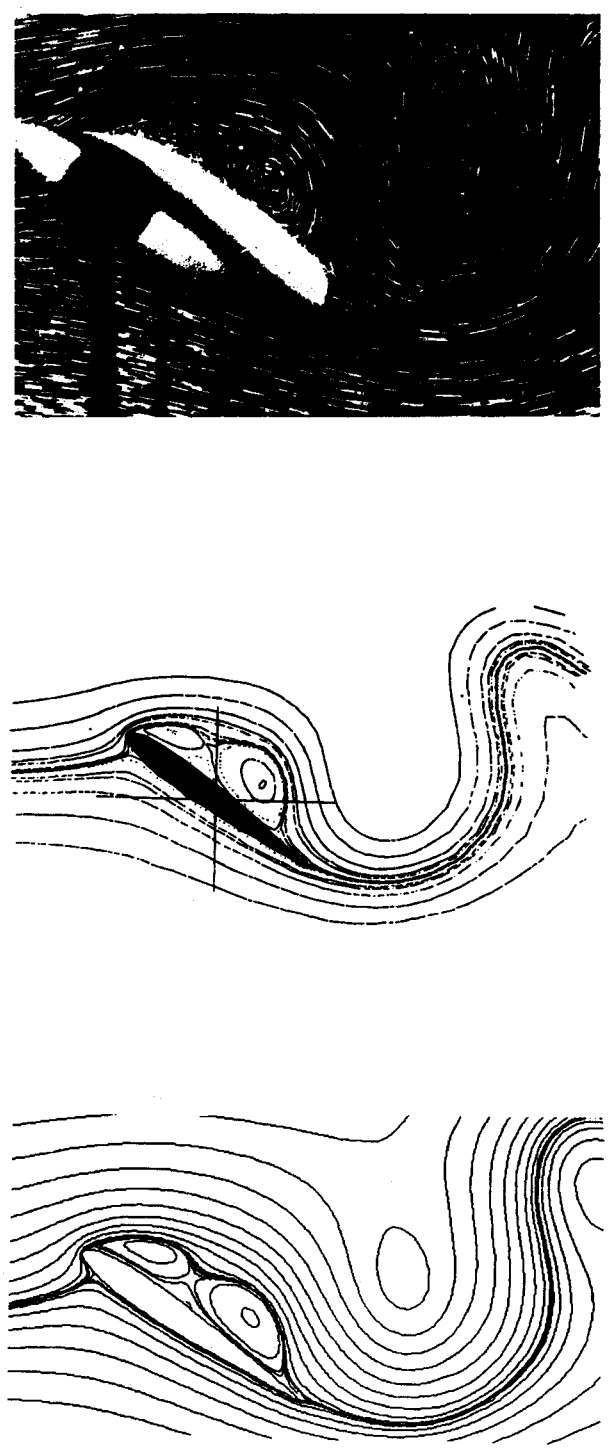

Figure 10. Comparison of flow structure between experimental visualization[21] and numerical results, $Re = 10^3$, $t = 10{\cdot}4$

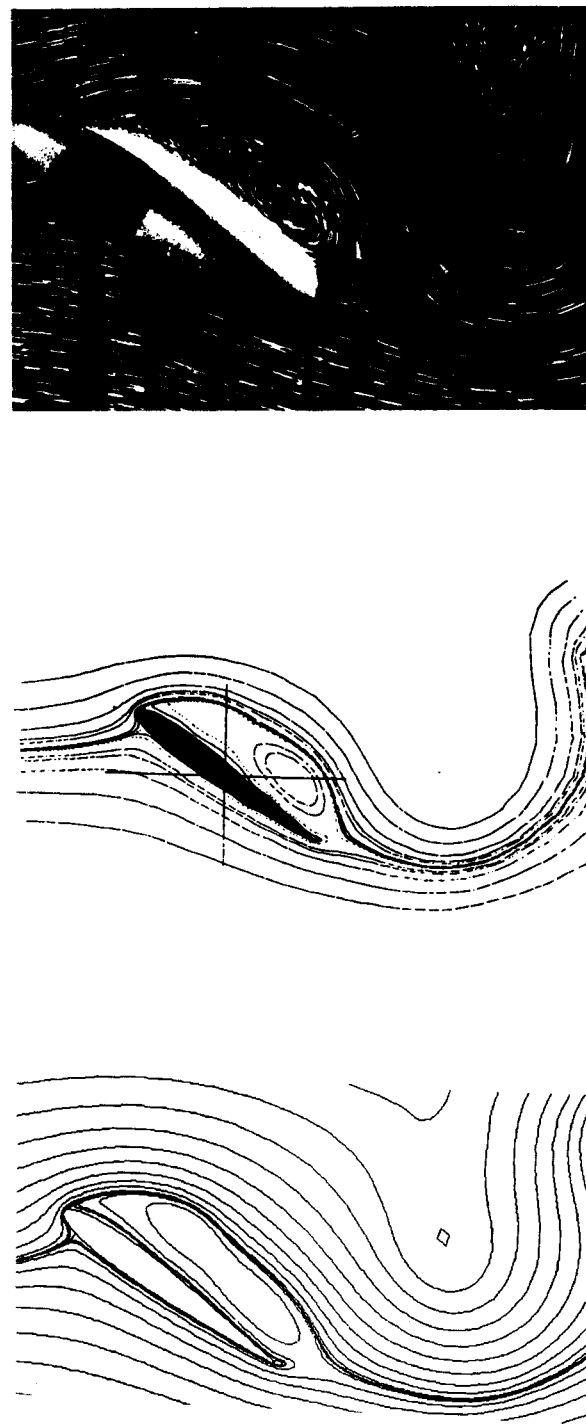

Figure 11. Comparison of flow structure between experimental visualization[21] and numerical results, $Re = 10^3$, $t = 11{\cdot}2$

6.2. *Re = 10,000*

The influence matrix techniques are often used for low Reynolds numbers. For high Reynolds numbers, owing to the linearization of the convection term, the stability of the numerical method requires the use of a more restrictive time step. In order to analyse the behaviour of the present method at high Reynolds numbers, the flow around the NACA 0012 aerofoil at a Reynolds number equal to 10^4 has been considered. The 'finite difference' subdomain is discretized with 81×161 nodes. Here the time step is chosen equal to 0·0005 to avoid instability. At this Reynolds number the experimental flow visualization points out the appearance of many microvortices along the surface of the aerofoil. The flow is less smooth, particularly in the separated zone. With a refined grid system these vortices are correctly reproduced in our numerical simulation. The repartition of the vorticity on the surface of the aerofoil, shown in Figures 12 and 13, confirms the presence of these microstructures. Despite the presence of 3D effects in the experimental visualization, the comparisons of the evolution of the flow with time between numerical results and experimental photographs from Laboratoire de Mécanique des Fluides de Poitiers (Pineau and Coutanceau, unpublished) are found to be fairly satisfactory, as shown in Figures 14–18.

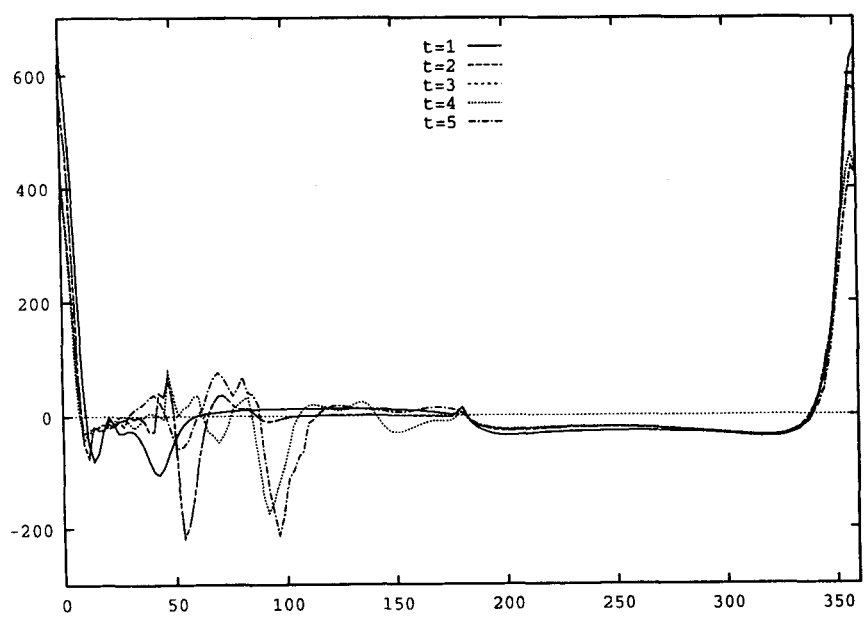

Figure 12. Repartition of vorticity on surface of aerofoil, $Re = 10^4$, $\alpha = 20°$

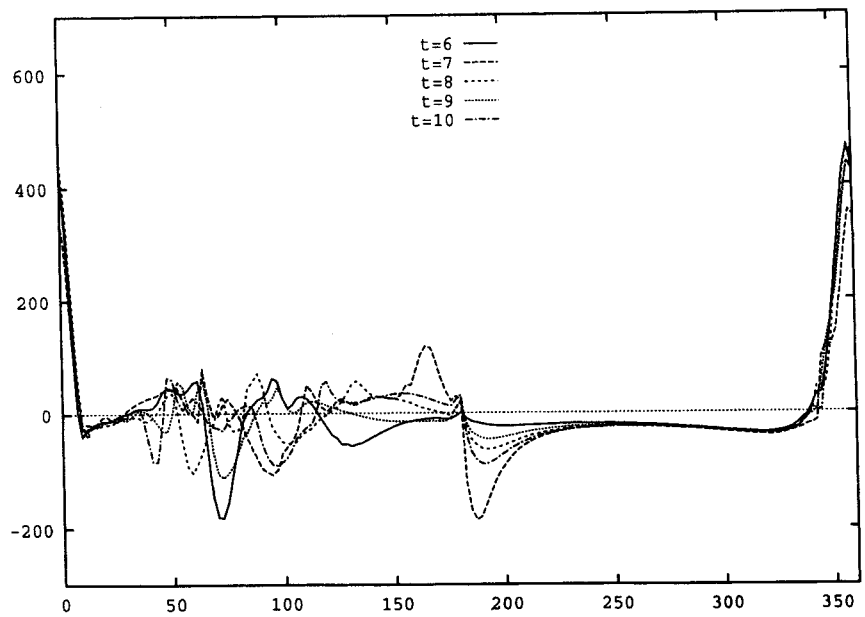

Figure 13. Repartition of vorticity on surface of aerofoil, $Re = 10^4$, $\alpha = 20°$

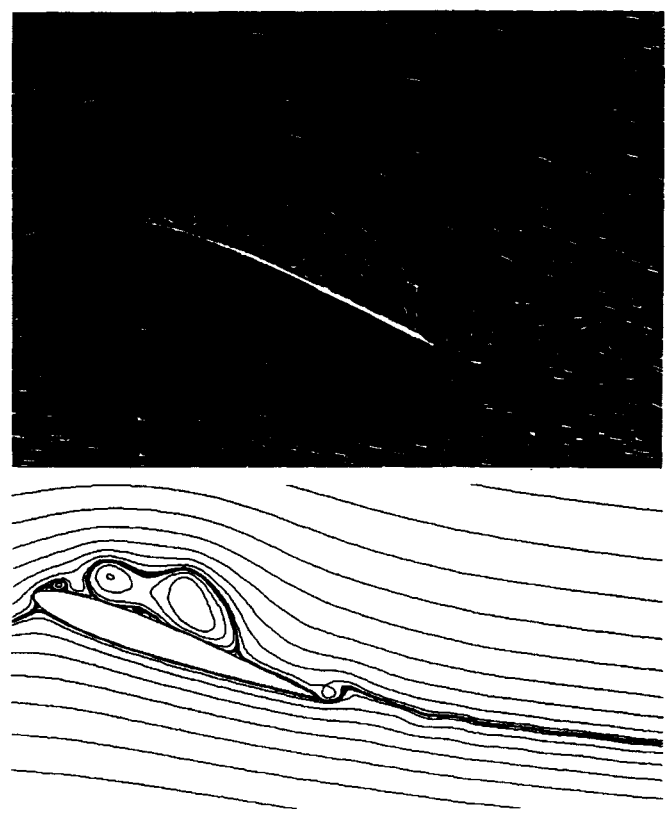

Figure 14. Comparison of flow structure between experimental visualization and numerical results, $Re = 10^4$, $t = 5$

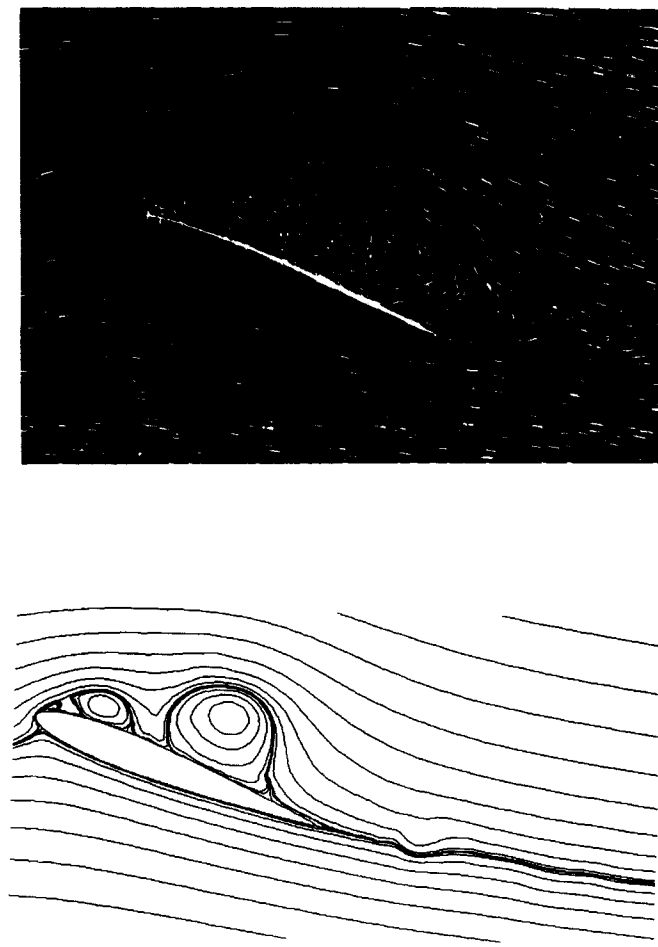

Figure 15. Comparison of flow structure between experimental visualization and numerical results, $Re = 10^4$, $t = 6$

Figure 16. Comparison of flow structure between experimental visualization and numerical results, $Re = 10^4$, $t = 7$

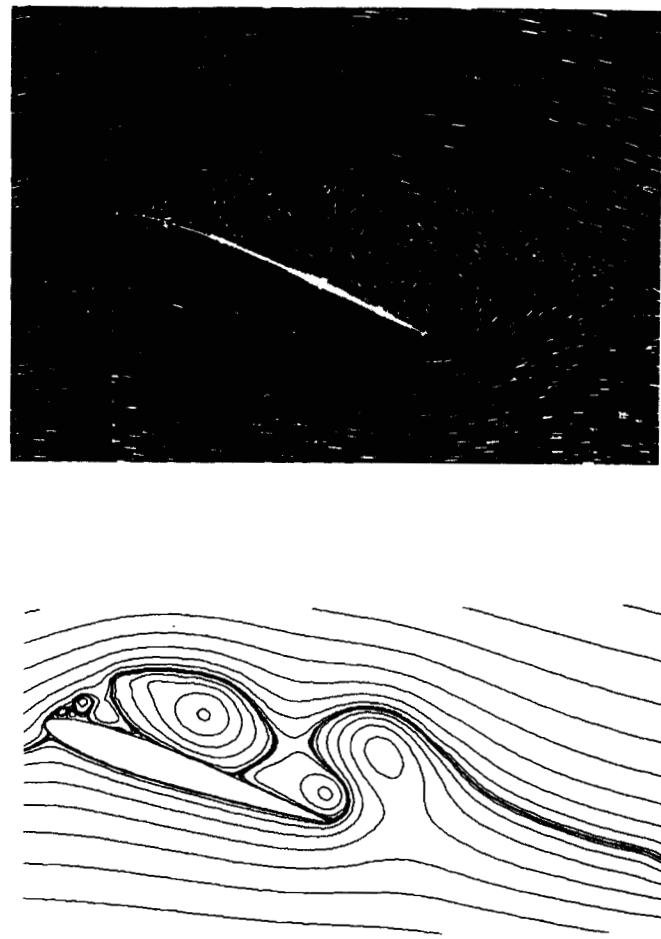

Figure 17. Comparison of flow structure between experimental visualization and numerical results, $Re = 10^4$, $t = 8$

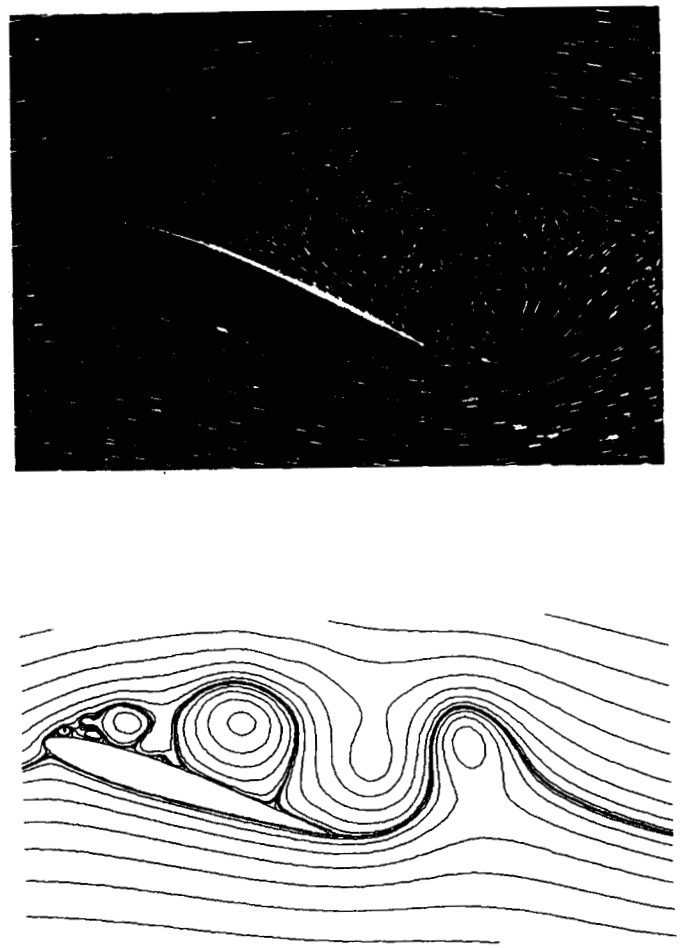

Figure 18. Comparison of flow structure between experimental visualization and numerical results, $Re = 10^4$, $t = 9$

7. CONCLUSIONS

In this paper we have presented a domain decomposition method using an influence matrix technique for the finite difference method to simulate external incompressible viscous flows. An original aspect of the present work lies in the coupling of the influence matrix technique and the uniformity condition of the pressure. Another contribution is that the coupling method is developed to treat high-Reynolds-number flows.

In order to increase the efficiency of the method, some technique improvements must be implemented. For example, the inner iteration of the finite difference method used to find the boundary value of ψ can be exploited using a variable relaxation parameter. In the vortex method the fast algorithm of Reference 22 can be used. The present approach can also be extended to multiple-moving-obstacle problems with or without heat transfer.

REFERENCES

1. A. Quarteroni, 'Domain decomposition methods for numerical solution of partial differential equations', *University of Minnesota Supercomputer Institute Res. Rep UMSI 90/246*, 1990.
2. P. Le Tallec, 'A direct introduction of some domain decomposition techniques for advection diffusion problems', *Proc. Fifth Int. Symp. on Domain Decomposition Methods for Partial Differential Equations*, SIAM, Norfolk, VA, 1991.
3. Y. Maday and A. T. Patera, 'Spectral element methods for the incompressible Navier–Stokes equations', in A. Noor and J. T. Oden (eds), *State of the Art Surveys in Computational Mechanics*, ASME, New York, 1989.
4. G. H. Cottet, 'Particle–grid domain decomposition methods for the Navier–Stokes equations in exterior domains', *Lect. Appl. Math.*, **28**, 103–117 (1991).
5. J. L. Guermond, S. Huberson and W. Z. Shen, 'Simulation of 2D external viscous flows by means of a domain decomposition method', *J. Comput. Phys.*, **108**, 343–352 (1993).
6. S. Huberson, A. Jolles and W. Z. Shen, 'Numerical simulation of incompressible viscous flows by means of particle methods', *Lect. Appl. Math.*, **28**, 369–384 (1991).
7. W. Z. Shen, 'Calcul d'écoulement tourbillonnaire visqueux incompressible par une méthode de couplage différences finies/ particulaire', *Thèse Doctorat*, Orsay, 1993.
8. R. Hockney, 'The potential calculation and some applications', *Methods Comput. Phys.*, **9**, 135 (1970).
9. W. Proskurowski and O. Widlund, 'On the numerical solution of Helmholtz's equation by the capacitance matrix method', *Math. Comput.*, **30**, 433 (1976).
10. W. Proskurowski, 'Numerical solution of Helmholtz's equation by implicit capacitance matrix methods', *ACM Trans. Math. Softw.*, **5**, 36 (1979).
11. A. Pares-Sierra and G. K. Vallis, 'A fast semi-direct method for the numerical solution of non-separable elliptic equations in irregular domains', *J. Comput. Phys.*, **82**, 398 (1989).
12. P. Le Quéré and T. Alziary de Roquefort, 'Sur une méthode spectrale semi-implicite pour la résolution des équations de Navier–Stokes d'un écoulement bidimensionnel visqueux incompressible', *C.R. Acad. Sci. Paris, Sér. II*, **294**, 941 (1982).
13. L. Quartapelle and A. Muzzio, in G. De Vahl Davis and C. Fletcher (eds), *Proc. Int. Symp. on Computational Fluid Dynamics*, Sydney, 1987, North-Holland, Amsterdam, 1988, p. 609.
14. L. Kleiser and U. Schumann, in E. H. Hirschel (ed.), *Proc. 3rd GAMM Conf. on Numerical Methods in Fluid Mechanics*, Köln, 1979, Vieweg, Wiesbaden, 1980, p. 165.
15. P. Le Quéré and T. Alziary de Roquefort, 'Computation of natural convection in two-dimensional cavities with Chebyshev polynomials', *J. Comput. Phys.*, **57**, 210 (1985).
16. O. Daube, 'Resolution of the 2D Navier–Stokes equations in velocity–vorticity form by means of an influence matrix technique', *J. Comput. Phys.*, **103**, 402–414 (1992).
17. S. C. R. Dennis and L. Quartapelle, 'Direct solution of the vorticity–stream function ordinary differential equations by a Chebyshev approximation', *J. Comput. Phys.*, **52**, 448 (1983).
18. L. Tuckermann, 'Divergence-free velocity fields in nonperiodic geometries', *J. Comput. Phys.*, **80**, 403 (1989).
19. J. M. Vanel, R. Peyret and P. Bontoux, in K. W. Morton and M. J. Baines (eds), *Proc. Int. Conf. on Numerical Methods for Fluid Dynamics*, Reading, 1985, Clarendon, New York, 1986, p. 463.
20. Y. Saad and M. H. Schultz, 'GMRES: a generalized minimal residual algorithm for solving nonsymmetric linear systems', *SIAM J. Sci. Stat. Comput.*, **7**, 856–869 (1986).
21. O. Daube, Ta Phuoc Loc, P. Monnet and M. Coutanceau, 'Ecoulement instationnaire décollé d'un fluide incompressible autour d'un profil: une comparaison théorie–expérience', *Conf. Proc. 386: Unsteady Aerodynamics–Fundamentals and Applications to Aircraft Dynamics*, 1985.
22. L. Greengard and V. Rokhlin, 'A fast algorithm for particle simulations', *J. Comput. Phys.*, **73**, 325–348 (1987).
23. A. J. Chorin, 'Numerical study of slightly viscous flow', *J. Fluid Mech.*, **57**, 785 (1973).

24. O. Daube and Ta Phuoc Loc, 'Etude numérique d'écoulements instationnaires de fluide visqueux incompressible autour de corps profilés par une méthode combinée d'ordre $O(h^4)$ et $O(h^2)$', *J. Méc.*, **17**, 651–678 (1978).
25. A. Jollès, 'Résolution des équations de Navier–Stokes par des méthodes particules/maillages', *Thèse Doctorat*, Paris, 1989.
26. Ta Phuoc Loc and R. Bouard, 'Numerical solution of the early stage of the unsteady viscous flow around a circular cylinder: a comparison with experimental visualization and measurements', *J. Fluid Mech.*, **160**, 93–117 (1985).
27. P. A. Raviart, 'An analysis of particle methods', in F. Brezzi (ed.), *Lecture Notes in Mathematics*, Vol. 1127, *Numerical Methods in Fluid Dynamics*, Springer, Berlin, 1985, pp. 243–324.
28. J. H. Williamson, 'Four cheap improvements to the particle–mesh code', *J. Comput. Phys.*, **41**, 256–269 (1981).